

Model for a Ferromagnetic Quantum Critical Point in a 1D Kondo Lattice

Yashar Komijani¹ and Piers Coleman^{1,2}

¹*Department of Physics and Astronomy, Rutgers University, Piscataway, New Jersey 08854, USA*

²*Department of Physics, Royal Holloway, University of London, Egham, Surrey TW20 0EX, United Kingdom*



(Received 17 November 2017; published 13 April 2018)

Motivated by recent experiments, we study a quasi-one-dimensional model of a Kondo lattice with ferromagnetic coupling between the spins. Using bosonization and dynamical large- N techniques, we establish the presence of a Fermi liquid and a magnetic phase separated by a local quantum critical point, governed by the Kondo breakdown picture. Thermodynamic properties are studied and a gapless charged mode at the quantum critical point is highlighted.

DOI: 10.1103/PhysRevLett.120.157206

Heavy fermion materials are a class of quantum system in which the close competition between magnetism and itineracy drives a wealth of novel quantum ground states, including hidden-order, strange, and quantum critical metals, topological insulators, and unconventional superconductivity [1,2]. The various entanglement mechanisms by which the localized magnetic moments correlate and transform heavy fermion materials provide an invaluable window on the governing principles needed to control and manipulate quantum matter.

An aspect of particular interest is the quantum criticality that develops when a second-order magnetic phase transition is tuned to absolute zero. In itinerant magnets, quantum phase transitions (QPTs) are understood in terms of the classic Slater-Stoner instabilities of Fermi liquids (FLs), described by the interaction of soft magnons with a Fermi surface, described in its simplest form by the Hertz-Millis-Moriya theory [3–5]. More recent treatments have examined the role of nonlocal interactions, mediated by the Fermi sea [6–8]; in itinerant ferromagnets, these interactions give rise to first-order QPTs, a feature in good accord with experiment. The nature of the quantum criticality in metals in which the magnetism has a localized moment character is less well understood, but is thought to involve a partial or complete Mott localization of the electrons, manifested in heavy fermion compounds as a breakdown of the Kondo effect and a possible collapse in the Fermi surface volume [9–15].

Most research into heavy fermion quantum criticality has focused on antiferromagnetic instabilities, often discussed as a competition between the Kondo screening of local moments and antiferromagnetism, driven by the Ruderman-Kittel-Kasuya-Yosida (RKKY) interaction [16–18]. However, there is now a growing family of heavy fermion systems, including α - and β -YbAlB₄ [19–21], YbNi₄P₂ [22], YbNi₃Al₉ [23], and CeRu₂Al₂B [24]. Unlike itinerant ferromagnets, these systems display

second-order quantum criticality, suggesting an important interplay of the Kondo effect with criticality [6,18,25].

These discoveries motivate us to examine quantum criticality in a Kondo lattice with ferromagnetic (FM) interactions. This affords many simplifications, for a uniform magnetization M commutes with the Hamiltonian $[M, H] = 0$ and is thus a conserved quantity, free from zero-point motion. Antiferromagnetic Kondo lattices are normally discussed in terms of a “global” phase diagram [10,14] with two axes—the Doniach parameter $x = T_K/J_H$, set by the ratio of the Kondo temperature T_K to the Heisenberg coupling J_H , and the frustration parameter y measuring the strength of magnetic zero-point fluctuations. The elimination of magnetic zero-point fluctuations allows us to focus purely on the x axis of the generalized phase diagram, and it becomes possible to study magnetic quantum criticality in a one-dimensional model.

Our model is motivated by the quasi-one-dimensional Yb structure of YbAlB₄, in which a chain of ferromagnetically coupled Yb spins hybridizes with multiple conducting planes of B atoms (Fig. 1) [26]. For simplicity, we treat each plane as an autonomous electron bath with a flat density of states, individually coupled via an antiferromagnetic Kondo coupling J_K , according to

$$H = \sum_j [H_c(j) + J_K \vec{S}_j \cdot \vec{\sigma}_j - J_H \vec{S}_j \cdot \vec{S}_{j+1}], \quad (1)$$

where \vec{S}_j is the spin at the j th site, coupled ferromagnetically to its neighbor with strength J_H . $H_c(j) = \sum_{\mathbf{p}} \epsilon_{\mathbf{p}} c_{\mathbf{p}\alpha}^\dagger(j) c_{\mathbf{p}\alpha}(j)$ describes the j th layer of electrons, coupled to the chain via its spin density $\vec{\sigma}_j = \psi_{j\alpha}^\dagger \vec{\sigma}_{\alpha\beta} \psi_{j\beta}$ at the chain, where \mathbf{p} is the momentum of the conduction electrons at the j th layer and $\psi_{j\alpha}^\dagger = \sum_{\mathbf{p}} c_{\mathbf{p}\alpha}^\dagger(j)$ creates an electron at the position of the magnetic moment j on the chain.

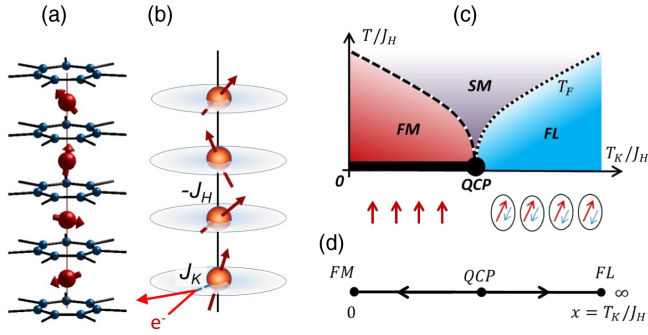


FIG. 1. (a) The quasi-1D structure of Yb local moments (red) in YbAlB₄ sandwiched between conducting B layers. (b) 1D model, showing ferromagnetically coupled local moments ($-J_H < 0$), each screened by a separate conduction electron sea (gray layers). (c) Phase diagram we find for the model as a function of T_K/J_H and temperature, showing a Fermi liquid and a 1D ferromagnetic regime, separated by a QCP, giving rise to a fan of strange metal (SM) behavior at high temperature. The Fermi temperature T_F vanishes at the QCP. The 1D FM only orders at zero temperature and is intrinsically quantum critical. (d) RG flow of transverse Ising model to which our model maps in the Ising limit.

At small $x = T_K/J_H$, the 1D chain is ferromagnetically correlated, developing true long-range order and breaking time-reversal symmetry at zero temperature, while at large x , it forms a paramagnet, where each spin is individually screened: in between, there is a sharp transition that we identify as a quantum critical point (QCP) [16,25]. This QCP has been demonstrated [27,28] in the Ising limit of this Kondo lattice at the Toulouse decoupling point [29], which permits bosonization of the Hamiltonian, mapping it [30] onto the transverse field Ising model, $H \rightarrow T_K \sum_n S_n^x + J_H^z \sum_n S_n^z S_{n+1}^z$. This model has a well-known RG flow [Fig. 1(d)] and a quantum phase transition at $J_H^z = T_K$ [31]. However, in this limit, the stable phases are gapped, and to gain a deeper insight into the physics of the QCP, we return to the Heisenberg limit.

Here instead, we use a large- N Schwinger boson approach that treats the magnetism in the Heisenberg limit, while also explicitly preserving the Kondo effect. Our method unifies the Arovas and Auerbach treatment of ferromagnetism [32] with the description of the Kondo problem by Parcollet *et al.* [33,34] and Coleman and co-workers [35,36]. An important aspects of this approach is the use of a multichannel Kondo lattice in which the spin S and the number of channels K is commensurate ($K = 2S$), allowing for a perfectly screened Kondo effect [36].

Figure 1(c) summarizes the key results. At large T_K/J_H , our method describes a FL phase with Pauli susceptibility $\chi \sim 1/T_F$ and a linear specific heat coefficient $\gamma = C/T \sim 1/T_F$. As x is reduced to a critical value x_c , the characteristic scale $T_F(x)$, determined from the magnetic susceptibility and linear specific heat coefficient [Figs. 2(c) and 2(d)], drops continuously to zero, terminating at a QCP. This suppression of T_F resembles the

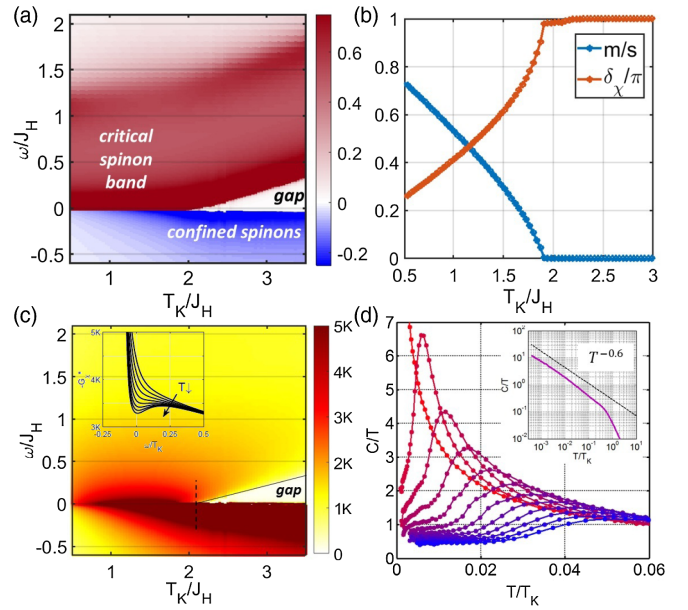


FIG. 2. (a) The spectral density of spinons $-G_B''(\omega + i\eta)$ for $k = s = 0.3$ as a function of T_K/J_H , shows the spinon band at positive energy and the Kondo-screened spins appearing as confined spinons at negative energy. The Kondo gap at large x shrinks linearly with lowering x , collapsing at about $x \approx 2$. (b) Zero temperature magnetization m/s (blue) and holon phase shift δ_χ/π (red) as a function of T_K/J_H . (c) The spectral density of holons $-G_\chi''(\omega + i\eta)$ as a function of T_K/J_H shows the critical mode at the QCP (inset). (d) Specific heat coefficient $\gamma(T) = C/T$ vs temperature as T_K/J_H is varied from 5 (blue) to 0.1 (red). The inset in (d) shows the power-law dependence of γ at the QCP.

Schrieffer mechanism for the reduction of the Kondo temperature in Hund's metals [37–40]. The large- N QCP is characterized by power-law dependences of the specific heat and local and uniform susceptibilities,

$$\chi(T) \sim \frac{1}{T}, \quad \chi_{\text{loc}}(T) \sim \frac{1}{T^{1-\alpha}}, \quad \frac{C}{T} \sim \frac{1}{T^\alpha}, \quad (2)$$

where the exponent $\alpha[s] < 1$ is function of the spin $s = 2S/N$. At still smaller x , the chain develops a fragile ferromagnetism that disappears at finite temperatures. Here $\chi \sim 1/T^2$ and $C/T \sim 1/\sqrt{T}$, characteristics of a critical 1D ferromagnetism. There are two notable aspects of the physics: first, the QCP exhibits an emergent critical charge fluctuation mode associated with Kondo breakdown, and second, the 1D ferromagnetic ground state is intrinsically quantum critical, transforming into a Fermi liquid with characteristic scale of order the Zeeman coupling, upon application of a magnetic field. This last feature is strongly reminiscent of the observed physics of β -YbAlB₄, a point we return to later.

Our large- N approach is obtained by casting the local moments as Schwinger bosons $S(j)_{\alpha\beta} = b_{j\alpha}^\dagger b_{j\beta}$, where $2S = n_b(j)$ is the number of bosons per site, each

individually coupled to a K channel conduction sea, with Hamiltonian

$$H = \sum_j \{H_{\text{FM}}(j) + H_K(j) + H_C(j) + \lambda_j [n_b(j) - 2S]\}, \quad (3)$$

where (scaling down coupling constants)

$$\begin{aligned} H_{\text{FM}}(j) &= -(J_H/N)(b_{j\alpha}^\dagger b_{j+1,\alpha})(b_{j+1,\beta}^\dagger b_{j\beta}), \\ H_K(j) &= -(J_K/N)(b_{j\alpha}^\dagger \psi_{ja\alpha})(\psi_{ja\beta}^\dagger b_{j\beta}), \\ H_C(j) &= \sum_{\mathbf{p}} \epsilon_{\mathbf{p}} c_{\mathbf{p}\alpha\alpha}^\dagger(j) c_{\mathbf{p}\alpha\alpha}(j), \end{aligned} \quad (4)$$

where λ_j is a Lagrange multiplier that imposes the constraint. Here we have adopted a summation convention, with implicit summations over the (greek) $\alpha \in [1, N]$ spin and (roman) $a \in [1, K]$ channel indices. In the calculations, we take $2S = K = sN$ for perfect screening, where s is kept fixed.

Next, we carry out the Hubbard-Stratonovich transformations

$$\begin{aligned} H_K(j) &\rightarrow [(b_{j\alpha}^\dagger \psi_{ja\alpha}) \chi_{ja} + \text{H.c.}] + \frac{N \bar{\chi}_{ja} \chi_{ja}}{J_K}, \\ H_{\text{FM}}(j) &\rightarrow [\bar{\Delta}_j (b_{j+1,\alpha}^\dagger b_{j,\alpha}) + \text{H.c.}] + \frac{N |\Delta_j|^2}{J_H}. \end{aligned} \quad (5)$$

The first line is the Parcollet-Georges factorization of the Kondo interaction, where the χ_{ja} are charged, spinless Grassman fields that mediate the Kondo effect in channel a . The second line is the Arovas-Auerbach factorization of the magnetic interaction in terms of the bond variables Δ_j describing the spinon delocalization. Both b and χ fields have nontrivial dynamics [33–36], with self-energies given by (see Supplemental Material [41])

$$\Sigma_\chi(\tau) = g_0(-\tau) G_B(\tau), \quad \Sigma_B(\tau) = -k g_0(\tau) G_\chi(\tau) \quad (6)$$

Here $G_\chi(\tau)$, $G_B(\tau)$, and $g(\tau)$ are the local propagators of the holons, spinons, and conduction electrons, respectively. The conduction electron self-energy is of order $O(1/N)$ and is neglected in the large- N limit, so that $g_0(\tau)$ is the bare local conduction electron propagator. The holon Green's function is purely local, given by $G_\chi(z) = [-J^{-1} - \Sigma_\chi(z)]^{-1}$, but the interesting new feature of our calculation is the delocalization of the spinons along the chain. Seeking uniform solutions where $\Delta_j = -\Delta$ and $\lambda_j = \lambda$, the spinons develop a dispersion $\epsilon_B(p) = -2\Delta \cos p$, with propagator $G_B(p, z) = [z - \epsilon_B(p) - \lambda - \Sigma_B(z)]^{-1}$. The momentum-summed *local* propagator is then

$$G_B(z) = \sum_p G_B(p, z) = \int \frac{d\epsilon_B \rho(\epsilon_B)}{z - \lambda - \epsilon_B - \Sigma_B(z)}, \quad (7)$$

where $\rho(\epsilon_B) = (2\pi\Delta)^{-1} [1 - (\epsilon_B/2\Delta)^2]^{-1/2}$ is the bare spinon density of states. Using Cauchy's theorem,

$$G_B(z) = \frac{1}{\Omega[z]} \frac{1}{\sqrt{1 - [\Omega(z)/2\Delta]^{-2}}}, \quad (8)$$

where $\Omega(z) \equiv z - \lambda - \Sigma_B(z)$ [41].

Stationarity of the free energy with respect to λ and Δ then leads to two saddle point equations

$$\begin{aligned} \int_{-\infty}^{+\infty} \frac{d\omega}{\pi} n_B(\omega) \text{Im}[G_B(\omega - i\eta)] &= s, \quad (9) \\ \frac{1 + \zeta \frac{\Delta^2}{J_H^2}}{J_H} &= \int \frac{d\omega}{2\pi\Delta^2} n_B(\omega) \text{Im}[\Omega(z) G_B(z)]_{z=\omega+i\eta}, \quad (10) \end{aligned}$$

which determine λ and J_H self-consistently.

In (10), we have added an additional $\zeta \frac{\Delta^2}{J_H^2}$, which stabilizes the quantum critical point. Schwinger boson mean-field theories suffer from weak first-order phase transitions upon development of finite Δ , due to fluctuation-induced attractive quartic $O(\Delta^4)$ terms in the effective action. This difficulty [42] has thwarted the study of quantum criticality with this method. These first-order transitions are actually a nonuniversal artifact of the way the large- N limit is taken, circumvented by adding a small repulsive biquadratic term $H'(j) = \zeta J_H (\vec{S}_j \cdot \vec{S}_{j+1})^2$ to the Hamiltonian. For an $\text{SU}(2)$ $S = 1/2$ moment, the biquadratic term can be absorbed into the Heisenberg interaction, but for the higher spin representations of the large- N expansion, it contributes a positive quartic correction $O(\zeta\Delta^4)$ to the effective action that restores the second-order phase transitions (at both zero and finite temperature) to the large- N limit [41]. In practice, a $\zeta \sim 0.001$ is sufficient to remove the first-order transition, so that Δ tunes linearly with J_H across the quantum critical point.

To find $G_B(\omega)$ and $G_\chi(\omega)$, we solve Eqs. (6)–(9) self-consistently on a linear and logarithmic grid. The entropy formula from [35,36] was used to compute the specific heat associated with these solutions [41].

In the Kondo limit ($T_K/J_H \gg 1$), the local moments are fully screened, forming a Fermi liquid; in the Schwinger boson scheme, the formation of Kondo singlets is manifested as a spectral gap $\Delta_g \sim T_K$ [36] in the spectrum of the spinons and holons, where $T_K = f(T_K^0, s)$ and $T_K^0 = D e^{-1/\rho J}$ is the Kondo temperature [Fig. 2(a)]. The opening of this gap effectively confines the spinon and conduction electron into a singlet bound state, leaving behind an elastic resonant scattering potential that satisfies the Friedel sum rule with phase shift $\delta = \pi/N$.

In the opposite ferromagnetic limit $T_K/J_H \ll 1$, the chain forms a fragile ferromagnet. In this case, the spinons are condensed in the ground state, but at finite temperatures, the spinon band is gapped: the constraint (9) ensures that the gap in the spectrum grows quadratically, $\Delta_b(T) \propto T^2$, and together with the quadratic dispersion, this leads to a free energy $F \propto T^{3/2}$, a critical susceptibility

$\chi \propto T^{-2}$, and a specific heat coefficient $C/T \propto T^{-1/2}$ [32,41] in agreement with Bethe ansatz [43–46]. The van Hove singularity of density of states means that the ferromagnet is fragile, so that the bosons only condense, developing true long-range order at absolute zero.

Figure 2 shows the evolution of properties between these two limits. As x is reduced, the spectral gap responsible for Fermi liquid behavior shrinks linearly to zero at the QCP at $x_c \approx 2$, an indication of Kondo breakdown. This suppression of the Kondo temperature with x is closely analogous to reduction of the Kondo temperature by Hund’s coupling [37,40,47], with $\Delta \sim J_H$ playing the role of the Hund’s coupling and the ratio ξ/a of the spin correlation length to the lattice spacing playing the role of the effective moment.

The ground-state ferromagnetic moment is given by

$$m = \lim_{T \rightarrow 0} \int_0^\infty \frac{d\omega}{\pi} n_B(\omega) \text{Im} G_B(\omega - i\eta), \quad (11)$$

which measures the residual positive-energy spinon population, which condenses at $T = 0$ [Fig. 2(b)]; m is zero in the fully screened state, and rises gradually to a maximum value $m = s = 2S/N$ in the ferromagnetic limit. Note that $m/s < 1$ indicates that the magnetic moment is partially screened by an incipient Kondo effect, which continues into the fragile magnetic phase.

Although our simple model does not allow us to examine the evolution of the Fermi surface, we can monitor the delocalization of heavy electrons by examining the phase shift of the holons $\delta_\chi = \text{Im} \ln[-G_\chi^{-1}(0 - i\delta)]$. The change in the number of delocalized heavy electrons Δn_f is related to the holon phase shift by the relation $\Delta n_f = \sum_a (\delta_\chi/\pi)$ [35,36], which is plotted as a function of x in Fig. 2(b). Although we do not observe a jump in Δn_f at the QCP, there is a sharp cusp in its evolution at $x = x_c$. One of the interesting aspects of our results is that the holon spectrum becomes critical at the QCP [Fig. 2(c), inset], signaling the emergence of a critical spinless charge fluctuation that accompanies the critical formation and destruction of singlets.

The specific heat coefficient $\gamma \equiv C/T = dS/dT$, plotted in Fig. 2(d) shows a “Schottky” peak at $T \sim T_F$ for large x (blue), which collapses to zero as $x \rightarrow x_c$ (red). At the QCP, $\gamma(T) \sim T^{-\alpha}$ follows a power law, where $\alpha[s]$ depends on the reduced spin $s = 2S/N$. In the calculations displayed here, $\alpha = 0.6$ for $s = 0.3$ [Fig. 2(d)]. In the magnetic phase, $\gamma \sim 1/\sqrt{T}$, again characteristic of 1D FM.

Figure 3(a) shows the dependence of the uniform spin susceptibility on x . In the Fermi liquid at large x (blue), there is a crossover from a Curie susceptibility $\chi \sim 1/T$ at high T to a Pauli susceptibility $\chi \sim 1/T_F$ at the Fermi temperature T_F . As x decreases, T_F decreases to zero and the susceptibility becomes critical. At the QCP, the susceptibility $\chi \sim 1/T$ follows a simple Curie law. For $x < x_c$, the susceptibility displays a $\chi \sim 1/T^2$ characteristic of 1D

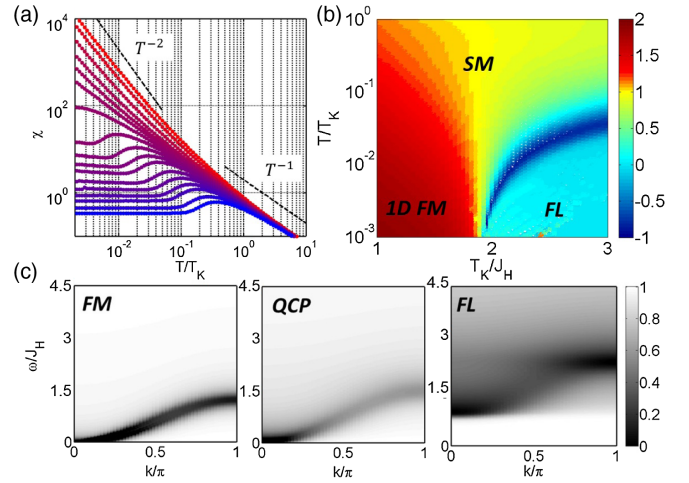


FIG. 3. (a) Uniform spin susceptibility χ as a function of temperature as T_K/J_H is varied from 0.1 (red) to 5 (blue). (b) The phase diagram obtained from the temperature exponent κ of susceptibility $\chi \sim T^{-\kappa}$ shows the Kondo breakdown induced by the Schrieffer suppression of the Fermi temperature and separated from the magnetic phase by a QCP. (c) Dynamical spin susceptibility in FL ($T_K/J_H = 3.6$), QCP (1.65), and FM (0.36) regimes, respectively.

FM. We use the dependence of the temperature exponent $\kappa = -d \log \chi / d \log T$ of the susceptibility on x and temperature to map out the phase diagram [Fig. 3(b)]. The dark blue stripe delineates the renormalized Fermi temperature of the Fermi liquid, showing its collapse to zero as $x \rightarrow x_c^+$. The corresponding evolution in the dynamical magnetic susceptibility $\chi''(q, \omega)$ of various phases is shown in Fig. 3(c). The sharp magnon band in the magnetic phase is smeared at the QCP, denoting fractionalization of the spins. The FL phase features a spectral gap, which is an artifact of the large- N method, as well as some remnants of the magnon band.

We have also studied the effect of a magnetic field [41]. While the Fermi liquid is robust, application of a small magnetic field to the QCP or the FM phase [48,49] immediately reinstates Fermi-liquid behavior with a scale T_B set by the Zeeman energy (at the QCP) or a combination of the spinon bandwidth and magnetic field (in the FM phase) [41]. The ferromagnetic phase is thus intrinsically quantum critical.

There are two interesting aspects of our Letter that merit further examination. First, we note that the intrinsic quantum criticality of the 1D FM phase in our model is reminiscent of $\beta - \text{YbAlB}_4$, raising the fascinating possibility that the critical FM in our one-dimensional model might be stabilized in higher dimensions by frustration. Second, we note that the Kondo breakdown at the QCP appears to involve a critical spinless charge degree of freedom. It is intriguing to speculate whether this might be an essential element of a future theory of heavy fermion quantum criticality.

The future extension of our work to antiferromagnetism will allow an exploration of the generalized phase diagram. Moreover, generalizations of the approach to higher dimensional systems are possible, using our approach as an impurity or cluster solver within a dynamical mean-field theory [50]. The effect of electron hopping between conduction layers, the resulting RKKY interaction it gives rise to, and possible nonuniform mean-field solutions are other interesting avenues for exploration.

This work was supported by a Rutgers University Materials Theory Postdoctoral Fellowship (Y.K.), and by NSF Grant No. DMR-1309929 (P.C.). We gratefully acknowledge discussions with Thomas Ayrál, Collin Broholm, Elio König, Satoru Nakatsuji, and Pedro Schlottmann.

-
- [1] F. Steglich and S. Wirth, *Rep. Prog. Phys.* **79**, 084502 (2016).
- [2] P. Coleman, *Introduction to Many-Body Physics* (Cambridge University Press, Cambridge, England, 2015).
- [3] J. A. Hertz, *Phys. Rev. B* **14**, 1165 (1976).
- [4] A. J. Millis, *Phys. Rev. B* **48**, 7183 (1993).
- [5] T. Moriya and T. Takimoto, *J. Phys. Soc. Jpn.* **64**, 960 (1995).
- [6] M. Brando, D. Belitz, F. M. Grosche, and T. R. Kirkpatrick, *Rev. Mod. Phys.* **88**, 025006 (2016).
- [7] M. A. Metlitski and S. Sachdev, *Phys. Rev. B* **82**, 075128 (2010).
- [8] X. Y. Xu, K. Sun, Y. Schattner, E. Berg, and Z. Y. Meng, *Phys. Rev. X* **7**, 031058 (2017).
- [9] P. Coleman, C. Ppin, Q. Si, and R. Ramazashvili, *J. Phys. Condens. Matter* **13**, R723 (2001).
- [10] Q. Si, S. Rabello, K. Ingersent, and J. L. Smith, *Nature (London)* **413**, 804 (2001).
- [11] T. Senthil, S. Sachdev, and M. Vojta, *Phys. Rev. Lett.* **90**, 216403 (2003).
- [12] S. Paschen, T. Lühmann, S. Wirth, P. Gegenwart, O. Trovarelli, C. Geibel, F. Steglich, P. Coleman, and Q. Si, *Nature (London)* **432**, 881 (2004).
- [13] H. Shishido, R. Settai, H. Harima, and Y. Onuki, *J. Phys. Soc. Jpn.* **74**, 1103 (2005).
- [14] P. Coleman and A. H. Nevidomskyy, *J. Low Temp. Phys.* **161**, 182 (2010).
- [15] Q. Si and F. Steglich, *Science* **329**, 1161 (2010).
- [16] S. Doniach, *Physica B+C (Amsterdam)* **91**, 231 (1977).
- [17] A. Schroder, G. Aeppli, R. Coldea, M. Adams, O. Stockert, H. Löhneysen, E. Bucher, R. Ramazashvili, and P. Coleman, *Nature (London)* **407**, 351 (2000).
- [18] H. v. Löhneysen, A. Rosch, M. Vojta, and P. Wölfle, *Rev. Mod. Phys.* **79**, 1015 (2007).
- [19] S. Nakatsuji, K. Kuga, Y. Machida, T. Tayama, T. Sakakibara, Y. Karaki, H. Ishimoto, S. Yonezawa, Y. Maeno, E. Pearson, G. G. Lonzarich, L. Balicas, H. Lee, and Z. Fisk, *Nat. Phys.* **4**, 603 (2008).
- [20] Y. Matsumoto, S. Nakatsuji, K. Kuga, Y. Karaki, N. Horie, Y. Shimura, T. Sakakibara, A. H. Nevidomskyy, and P. Coleman, *Science* **331**, 316 (2011).
- [21] Y. Matsumoto, S. Nakatsuji, K. Kuga, Y. Karaki, Y. Shimura, T. Sakakibara, A. H. Nevidomskyy, and P. Coleman, *J. Phys. Conf. Ser.* **391**, 012041 (2012).
- [22] A. Steppke, R. KÜchler, S. Lausberg, E. Lengyel, L. Steinke, R. Borth, T. Lühmann, C. Krellner, M. Nicklas, C. Geibel, F. Steglich, and M. Brando, *Science* **339**, 933 (2013).
- [23] R. E. Baumbach, H. Chudo, H. Yasuoka, F. Ronning, E. D. Bauer, and J. D. Thompson, *Phys. Rev. B* **85**, 094422 (2012).
- [24] R. Miyazaki, Y. Aoki, R. Higashinaka, H. Sato, T. Yamashita, and S. Ohara, *Phys. Rev. B* **86**, 155106 (2012).
- [25] S. J. Yamamoto and Q. Si, *Proc. Natl. Acad. Sci. U.S.A.* **107**, 15704 (2010).
- [26] A. H. Nevidomskyy and P. Coleman, *Phys. Rev. Lett.* **102**, 077202 (2009).
- [27] A. M. Lobos, M. A. Cazalilla, and P. Chudzinski, *Phys. Rev. B* **86**, 035455 (2012).
- [28] A. M. Lobos and M. A. Cazalilla, *J. Phys. Condens. Matter* **25**, 094008 (2013).
- [29] G. Toulouse, *C R Acad. Bulg. Sci.* **268**, 1200 (1969).
- [30] Y. Komijani and P. Coleman (to be published).
- [31] S. Sachdev, *Quantum Phase Transitions*, 2nd ed. (Cambridge University Press, Cambridge, England, 2011).
- [32] D. P. Arovas and A. Auerbach, *Phys. Rev. B* **38**, 316 (1988).
- [33] O. Parcollet and A. Georges, *Phys. Rev. Lett.* **79**, 4665 (1997).
- [34] O. Parcollet, A. Georges, G. Kotliar, and A. Sengupta, *Phys. Rev. B* **58**, 3794 (1998).
- [35] P. Coleman, I. Paul, and J. Rech, *Phys. Rev. B* **72**, 094430 (2005).
- [36] J. Rech, P. Coleman, G. Zarand, and O. Parcollet, *Phys. Rev. Lett.* **96**, 016601 (2006).
- [37] J. R. Schrieffer, *J. Appl. Phys.* **38**, 1143 (1967).
- [38] A. I. Larkin and V. I. Mel'nikov, *Sov. Phys. JETP* **34**, 656 (1972).
- [39] K. Haule and G. Kotliar, *New J. Phys.* **11**, 025021 (2009).
- [40] A. H. Nevidomskyy and P. Coleman, *Phys. Rev. Lett.* **103**, 147205 (2009).
- [41] See Supplemental Material at <http://link.aps.org/supplemental/10.1103/PhysRevLett.120.157206> for further details and proofs of statements.
- [42] T. N. De Silva, M. Ma, and F. C. Zhang, *Phys. Rev. B* **66**, 104417 (2002).
- [43] P. Schlottmann, *Phys. Rev. Lett.* **54**, 2131 (1985).
- [44] P. Schlottmann, *Phys. Rev. B* **33**, 4880 (1986).
- [45] M. Takahashi and M. Yamada, *J. Phys. Soc. Jpn.* **54**, 2808 (1985).
- [46] M. Takahashi, *Phys. Rev. Lett.* **58**, 168 (1987).
- [47] I. Okada and K. Yosida, *Prog. Theor. Phys.* **49**, 1483 (1973).
- [48] P. Coleman and C. Pépin, *Phys. Rev. B* **68**, 220405 (2003).
- [49] P. Coleman and I. Paul, *Phys. Rev. B* **71**, 035111 (2005).
- [50] A. Georges, G. Kotliar, W. Krauth, and M. J. Rozenberg, *Rev. Mod. Phys.* **68**, 13 (1996).